# Structural and Biochemical Characterization of a Fluorogenic Rhodamine-Labeled Malarial Protease Substrate[†]

Michael J. Blackman,*[,‡] John E. T. Corrie,[‡] John C. Croney,[§] Geoff Kelly,[‡] John F. Eccleston,[‡] and David M. Jameson[§]

*National Institute for Medical Research, The Ridgeway, Mill Hill, London NW7 1AA, U.K., and Department of Cell and Molecular Biology, John A. Burns School of Medicine, University of Hawaii, Honolulu, Hawaii 96822-2319*

*Received June 27, 2002; Revised Manuscript Received August 8, 2002*

ABSTRACT: Activation of the proenzyme form of the malarial protease PfSUB-1 involves the autocatalytic cleavage of an Asp−Asn bond within the internal sequence motif [215]LVSADNIDIS[224]. A synthetic decapeptide based on this sequence but with the N- and C-terminal residues replaced by cysteines (Ac-CVSADNIDIC-OH) was labeled with 5- or 6-isomers of iodoacetamidotetramethylrhodamine (IATR). The doubly labeled peptides have low fluorescence because of ground-state, noncovalent dimerization of the rhodamines. Cleavage of either peptide by recombinant PfSUB-1 results in dissociation of the rhodamine dimers, which abolishes the self-quenching and consequently leads to an ∼30-fold increase in the fluorescence. This spectroscopic signal provides a continuous assay of proteolysis, enabling quantitative kinetic measurements to be made, and has also enabled the development of a fluorescence-based assay suitable for use in high-throughput screens for inhibitors of PfSUB-1. The structure of the rhodamine dimer in the 6-IATR-labeled peptide was shown by NMR to be a face-to-face stacking of the xanthene rings. Time-resolved fluorescence measurements suggest that the doubly labeled peptides exist in an equilibrium consisting of rhodamines involved in dimers (closed forms) and rhodamines not involved in dimers (open forms). These data also indicate that the rhodamine dimers fluoresce and that the associated lifetimes are subnanosecond.

Malaria is a major human disease for which existing drugs are relatively unsatisfactory and prone to development of resistance. In the course of a program to study malarial proteases, in part for their potential as novel drug targets (*1*), a fluorogenic substrate was required for the protease PfSUB-1, a subtilisin-like serine protease expressed in the merozoite stage of the human malaria parasite *Plasmodium falciparum*. Merozoites of *P. falciparum* invade and replicate within red blood cells, and invasion is known to require the activity of parasite serine proteases (*1*). Recombinant, enzymatically active PfSUB-1 has been produced using the baculovirus/insect cell system (*2, 3*). Immediately following translation, PfSUB-1 undergoes an autocatalytic activation step in which the proenzyme is cleaved at an internal Asp−Asn bond within the motif [215]LVSADNIDIS[224]. An N-acetylated synthetic decapeptide (Ac-LVSADNIDIS-OH) based on this site is cleaved at the same bond by either recombinant PfSUB-1 or authentic parasite-derived enzyme (*2, 3*).

To utilize this peptide as a fluorogenic substrate, we were attracted to the work of other groups who had found that peptides of between 4 and 20 residues labeled at both the

N- and C-termini with tetramethylrhodamine show substantial quenching of the rhodamine fluorescence. The quenching is attributed to intramolecular dimerization of the dyes, and cleavage of the sequence by a protease of appropriate specificity relieves the quenching by allowing the dye molecules to dissociate (*4, 5*). The dimerization, a typical property of rhodamine dyes that is normally observed at high dye concentration (e.g., refs *6−8*), is promoted by the high local concentration enforced by the linking peptide. In previous work, rhodamines were attached to the peptides either through amino or thiol peptide groups. Here we replaced the N- and C-terminal residues of the decapeptide by cysteines (Ac-CVSADNIDIC-OH) and alkylated both cysteine side chains with 5- or 6-IATR[1] (Figure 1). We were pleased in early experiments to find that cleavage of the 6-IATR-labeled peptide, either specifically by PfSUB-1 or nonspecifically by Pronase, resulted in a large increase in rhodamine fluorescence. This result prompted us to make a more detailed characterization of the labeled peptide, initially

[1] Abbreviations: Abz, 2-aminobenzoyl; DABCYL, 4-(4-dimethylaminophenylazo)benzoic acid; DMF, *N,N*-dimethylformamide; DMSO, dimethyl sulfoxide; 6-CATR, 6-chloroacetamidotetramethylrhodamine; 5- or 6-IATR, 5- or 6-iodoacetamidotetramethylrhodamine; EDANS, 5-(2-aminoethylamino)naphthalene-1-sulfonic acid; FRET, fluorescence resonance energy transfer; NOESY, nuclear Overhauser effect spectroscopy; pepF1-5R, peptide Ac-CVSADNIDIC-OH labeled at the N- and C-terminal cysteines with 5-IATR; pepF1-6R, peptide Ac-CVSADNIDIC-OH labeled at the N- and C-terminal cysteines with 6-IATR; pHMB, *p*-hydroxymercuribenzoate; RP-HPLC, reversed-phase high-performance liquid chromatography; TCEP, tris(carboxyethyl)phosphine; TFA, trifluoroacetic acid; TOCSY, total correlation spectroscopy.

FIGURE 1: Structure and numbering system for iodoacetamidorhodamine compounds used in this study.

to clarify the nature of the rhodamine−rhodamine dimer, and we now report a range of biophysical studies. Using NMR spectroscopy we have studied the relative orientation of the rhodamine monomers in their dimerized state and have shown that the peptide chain has an unstructured conformation in solution. We have investigated the underlying photophysical behavior by steady-state and time-resolved fluorescence measurements and carried out enzymological measurements to define limits for the cleavage parameters. These studies provide a strong foundation for use of the present labeled peptide in high-throughput screening assays for inhibitors of PfSUB-1 but also illuminate the likely generality of this approach to measuring peptidase activity.

## EXPERIMENTAL PROCEDURES

*Materials*. The peptide Ac-CVSADNIDIC-OH was synthesized in-house by standard solid-phase Fmoc chemistry. Recombinant PfSUB-1 (*2*, *3*) and 5- and 6-IATR (*9*) were prepared as previously described. Pronase and NP-40 detergent were from Boehringer Mannheim. TCEP was from Molecular Probes (Eugene, OR); other biochemicals and DMSO-$d_6$ were from Sigma.

*Synthesis of Labeled Peptides*. A solution of Ac-CVSAD-NIDIC-OH (10 mg, 9.1 $\mu$mol) in DMF (910 $\mu$L) was added to 50 mM Tris-HCl, pH 7.6 (8.2 mL), followed by TCEP from a freshly prepared 40 mM aqueous solution to a final concentration of 2 mM (i.e., 2-fold molar excess over peptide). The mixture was incubated under nitrogen at 21 °C for 18 h; then the reduced peptide was purified by RP-HPLC on a Vydac 10 mm × 25 cm semipreparative C$_{18}$ column that was eluted at 4.7 mL min$^{-1}$ with a 4.5−31.5% (v/v) gradient of acetonitrile in 0.1% TFA over 30 min. The fractions containing the reduced peptide were lyophilized, taken up in DMF (910 $\mu$L), and added to degassed 50 mM Tris-HCl, pH 7.6, containing 0.1 mM EDTA (7.3 mL), and then immediately supplemented with 6-IATR (910 $\mu$L of 21.3 mM solution in DMF) with continuous stirring. After overnight incubation under nitrogen in the dark at room temperature, the reaction was quenched with 2 M sodium 2-mercaptoethanesulfonate (280 $\mu$L). After a further 2 h incubation at room temperature, the crude reaction mixture was applied to a G10 Sephadex column [1.6 × 65 cm; equilibrated in 30% (v/v) aqueous acetic acid] and eluted at 4 mL h$^{-1}$ with the same solvent, collecting 4 mL fractions. Aliquots (20 $\mu$L) of individual fractions were analyzed on a Vydac 4.6 mm × 25 cm C$_{18}$ reversed-phase column, eluted at 1 mL min$^{-1}$ with a 4.5−58.5% (v/v) gradient of acetonitrile in 0.1% TFA over 60 min. Samples of the reaction products were collected manually, dried under vacuum,

dissolved in 60% (v/v) acetonitrile plus 0.1% formic acid, and analyzed by electrospray mass spectrometry on a Micromass Platform single quadrupole mass spectrometer (Micromass, Altringham, U.K.). The first peak to elute from the G10 column contained predominantly the expected, doubly labeled peptide, called pepF1-6R (observed mass 1978.0 Da, calculated mass 1976.9 Da). The relevant fractions were pooled and further purified on a Vydac 10 mm × 25 cm semipreparative C$_{18}$ column, eluted at 4.7 mL min$^{-1}$ over 30 min with a 22.5−36% (v/v) gradient of acetonitrile in 0.1% TFA. The purified pepF1-6R was lyophilized, redissolved in DMSO (or DMSO-$d_6$ for NMR measurements) at a concentration of 10.5 mM, and stored over desiccant in the dark at −20 °C. This material was used for the NMR and kinetic measurements. However, analytical RP-HPLC analysis showed that it contained 10% of another rhodamine-containing species that was removed on a Vydac 4.6 mm × 25 cm C$_{18}$ reversed-phase column, eluted at 1 mL min$^{-1}$ with a 4.5−58.5% (v/v) gradient of acetonitrile in 0.1% TFA over 60 min. The resulting purified product, estimated to be more than 99% pure, was used for the steady-state and time-resolved fluorescence measurements.

A similar protocol was followed for preparation of the peptide labeled with 5-IATR (called pepF1-5R).

*Specificity of PepF1-6R Cleavage by Recombinant PfSUB-1*. All concentrations were determined from the rhodamine absorption at 528 nm, based on $\epsilon_{528}$ 52000 M$^{-1}$ cm$^{-1}$ (*9*). Throughout the text, where concentrations refer to the doubly labeled peptides, they are given in terms of the peptide concentration, i.e., half that of the dye. Solutions of labeled peptide were prepared by dilution from stock DMSO solutions into protease digestion buffer [20 mM Tris-HCl, 50 mM NaCl, 12 mM CaCl$_2$, 0.05% NP-40 (w/v), pH 7.6]. It was necessary to include NP-40 detergent in all buffers that contained the labeled peptides to avoid nonspecific adsorption to glass and plastic ware. A sample of pepF1-6R (20 $\mu$M in digestion buffer) was supplemented with recombinant PfSUB-1 (~40 nM protein) and incubated at 37 °C to allow partial hydrolysis of the peptide. The sample was then fractionated by RP-HPLC fractionation on a Vydac 4.6 mm × 25 cm C$_{18}$ column, eluted at 1 mL min$^{-1}$ with a 4.5−58.5% (v/v) gradient of acetonitrile in 0.1% TFA over 60 min. Eluted products were collected and analyzed by electrospray mass spectrometry as described above.

*NMR Spectroscopy*. NMR spectra of pepF1-6R were recorded at 800 MHz proton frequency on a Varian Inova spectrometer. Spectra were recorded in 10% DMSO-$d_6$−20 mM sodium acetate, pH 5.0 (H$_2$O:D$_2$O 9:1) at 25 °C. The low solubility in this solvent system limited the sample concentration to 50 $\mu$M and necessitated the use of the highest available field. Two-dimensional TOCSY (*10*) and NOESY (*11*) spectra were recorded, employing WATER-GATE (*12*) for solvent suppression. A mixing time of 70 ms was used in the TOCSY spectrum, while separate NOESY spectra were recorded with mixing times of 200, 400, 600, and 800 ms. Quadrature detection in indirect dimensions was achieved using the States procedure (*13*). Spectra were referenced with respect to the residual water resonance at 4.75 ppm and were processed and analyzed using the nmrPipe/nmrDraw package (*14*). Molecular modeling was performed using InsightII (Accelrys Inc., Princeton, NJ). Control one-dimensional NOE spectra of 6-chloroac-

etamidotetramethylrhodamine (*9*) were obtained for a 2 mM solution in CDCl$_3$−MeOH-*d*$_4$ (7:3 v/v) at 600 MHz on a Varian Unity spectrometer.

*Absorption Spectroscopy.* Solutions of pepF1-5R and pepF1-6R were prepared at ∼2 *μ*M concentration by dilution from stock DMSO solutions into protease digestion buffer. Portions (4 mL) of each solution were treated with an aliquot of Pronase (16 *μ*L of 1 mg mL$^{-1}$ in the same buffer) and incubated at room temperature for 30 min. Absorbance spectra of these solutions and of the corresponding labeled peptides prior to Pronase treatment were recorded (Shimadzu UV-2401PC spectrophotometer). Absorbance spectra of intact peptides were measured similarly for solutions in the range pH 5−10.

*Fluorescence Measurements.* Steady-state fluorescence emission spectra were recorded with an ISS PC1 spectrofluorometer (ISS Inc., Champaign, IL) using a 3 × 3 mm path-length cell. Spectra were recorded with excitation through a polarizer at 54.7° to the vertical, and emission was viewed through a vertical polarizer. These spectra were corrected for the wavelength dependence of the photomultiplier response using the ISS data correction files. Technical emission spectra were also recorded without the use of polarizers or correction for monochromator or photomultiplier responses.

Time-resolved fluorescence measurements were made using an ISS K2 multifrequency phase and modulation spectrophotometer. The intensity of the excitation light (501 nm from a Spectra-Physics 2045 argon ion laser) was sinusoidally modulated over the range 20−250 MHz, and the phase shift and relative intensity modulation of the emission with respect to the excitation were determined (*15*). To circumvent polarization artifacts, the excitation light was polarized parallel to the vertical laboratory axis, and the emission was viewed through a polarizer oriented at 54.7° (*16*). The phase and modulation data as a function of the modulation frequency of the excitation light were analyzed as discrete exponential decays (*17*). Emission at wavelengths longer than 530 nm was measured through a Schott 087 long-pass filter.

Kinetic measurements of enzyme activity were made in an SLM 8000 instrument with excitation at 550 nm and emission monitored through a Wratten 22 filter. Experimental conditions are given in the legends to Figures 7 and 8.

*Multiwell Fluorescence Assay.* Purified recombinant PfSUB-1 at a range of concentrations in digestion buffer was dispensed in 50 *μ*L aliquots into wells of white 96-well microtiter plates (FluoroNunc, NUNC). Wells were supplemented with either 0.5 *μ*L of 100 mM pHMB or 0.5 *μ*L of water; then the plates were placed on a rotary shaker and mixed at room temperature for 30 min prior to the addition of 50 *μ*L of a solution of pepF1-6R at various concentrations in digestion buffer. Plates were sealed and incubated at 37 °C for 18 h before being read on a Perkin-Elmer LS-50B luminescence spectrometer fitted with a LS50B WPR multiplate reader accessory. Measurements were performed at excitation wavelength 552 nm, slit width 4 nm, and emission wavelength 580 nm, slit width 2.5 nm. Data collection was managed using Perkin-Elmer FL WinLab software.
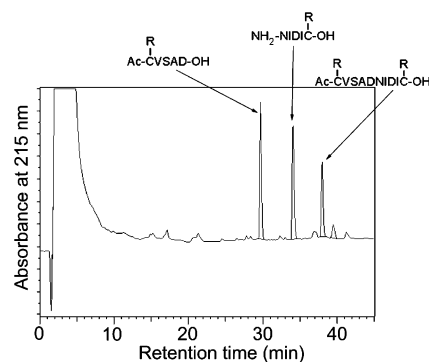


FIGURE 2: Reversed-phase HPLC fractionation of pepF1-6R following limited digestion with recombinant PfSUB-1. The identities of the three dominant eluted species, as determined by electrospray mass spectrometry, are indicated. Cysteine side chains modified using 6-IATR are shown (−R).

## RESULTS

*PepF1-6R Is a Substrate for PfSUB-1.* For all protease digestion experiments, pepF1-6R was diluted from a DMSO stock solution directly into protease digestion buffer, maintaining the final DMSO concentration at ≤5% (v/v). Addition of Pronase or purified recombinant PfSUB-1 resulted in a large, time-dependent increase in fluorescence (see below). Incubation with PfSUB-1 that had been pretreated with 1 mM pHMB, a potent inhibitor of the enzyme (*2, 3*), produced no fluorescence increase. A sample of pepF1-6R which had been partially digested with PfSUB-1 was subjected to RP-HPLC fractionation. In addition to a peak with retention time 37.9 min corresponding to residual pepF1-6R, two large new fluorescent peaks were present, with retention times of 29.6 and 34.0 min (Figure 2). Mass spectrometry showed that these peaks corresponded to the expected products of cleavage at the Asp−Asn bond; the measured masses of the products were 977.5 Da (the N-terminal cleavage product, calculated mass 977.5 Da) and 1018.4 Da (the C-terminal cleavage product, calculated mass 1018.5 Da).

*Absorption and Fluorescence Spectra of PepF1-5R and PepF1-6R.* Panels a and b of Figure 3 show the visible absorption spectra of the labeled peptides before and after digestion with Pronase. Total rhodamine concentrations are identical within each pair of samples, and the spectra cross exactly at 528 nm, previously shown to be the isosbestic point for the monomer−dimer equilibrium of simple 5- and 6-IATR derivatives (*9*). The spectra of the intact labeled peptides for the two isomers show marked differences in the relative intensities of the low- and high-wavelength bands at 518 and 549 nm [absorbance ratios (518/549) for pepF1-5R and -6R were 1.76 and 2.77, respectively] that are characteristic of dye dimerization (*6−8, 18*). Absorbance spectra of pepF1-6R were identical over the pH range 5−10 (data not shown), suggesting that the rhodamine interaction was unaffected within these limits. The spectra of the pepF1-5R and -6R also show differences in the mid-UV region. The Pronase-treated sample of pepF1-5R has a peak at ∼353 nm, while in the intact peptide the peak is significantly broadened and centered at ∼370 nm. In contrast, the spectra of cleaved and intact pepF1-6R are much more similar to one another within this region, with only slight broadening and a red shift from ∼353 to ∼355 nm between the cleaved and intact peptide (see insets to Figure 3a,b). These differ-
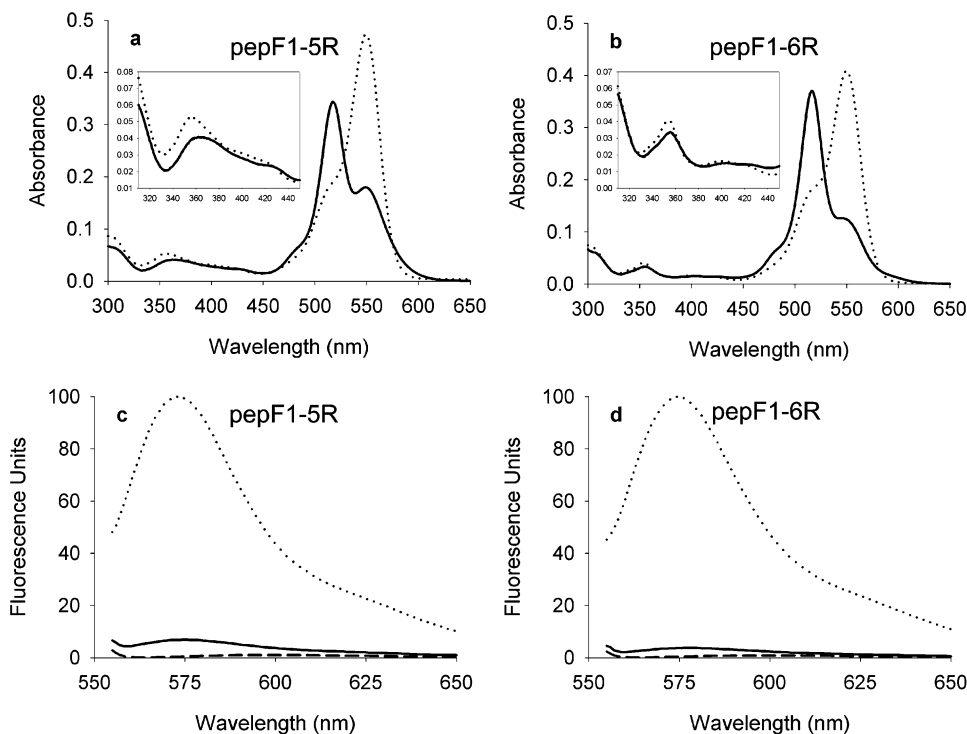
FIGURE 3: (a, b) Absorption spectra of pepF1-5R and pepF1-6R, respectively, each at ∼2 μM concentration. Solid lines are for the intact peptides, and dotted lines are for the same solutions after digestion with Pronase. Note that cleavage of the peptides by recombinant PfSUB-1 resulted in identical spectra (not shown). The inserts show expansions of these absorption spectra to highlight the mid-UV region. (c, d) Corrected emission fluorescence spectra of pepF1-5R and pepF1-6R, respectively, each at ∼0.5 μM concentration. Solid and dotted lines are as in (a) and (b), and the dashed lines are for buffer plus NP-40 alone.

ences likely reflect differences in the geometry and/or the association/dissociation kinetics of the rhodamine dimers in the two intact peptides, but we have not investigated this further.

The corrected fluorescence emission spectra with excitation at 550 nm of intact and cleaved pepF1-5R and pepF1-6R together with the buffer containing NP-40 are shown in panels c and d of Figure 3, respectively. For both peptides there is a large enhancement in emission intensity upon cleavage. However, there is also a weak fluorescence signal arising from an impurity in the NP-40 with an emission maximum at 595 nm. The emission maximum of uncleaved pepF1-5R is 580 nm, and that of the cleaved peptide is 575 nm. This difference can be attributed to the larger effect of the NP-40 fluorescence on the weakly fluorescent uncleaved peptide. At 575 nm the enhancement in intensity is 18-fold, but after correction for buffer fluorescence rises to 21-fold. Integrating the emission spectum between 555 and 650 nm gives an enhancement of 15-fold and 22-fold before and after taking the NP-40 fluorescence into account.

In the case of pepF1-6R, the emission maxima of uncleaved and cleaved peptide were at 575 and 573 nm, respectively. The enhancement at 573 nm was 23-fold before and 32-fold after correction for the NP-40 fluorescence. The equivalent values obtained by integrating the spectrum between 555 and 650 nm were 19-fold and 33-fold. Similar results were obtained for spectra uncorrected for polarization artifacts or photomultiplier spectral response. For example, pepF1-6R gave an increase of 30-fold, either at 573 nm alone or in the integrated spectrum after taking the NP-40 fluorescence into account.

*Conformation of PepF1-6R*. Figure 4 shows a selected region of the NOESY spectrum of intact pepF1-6R in which
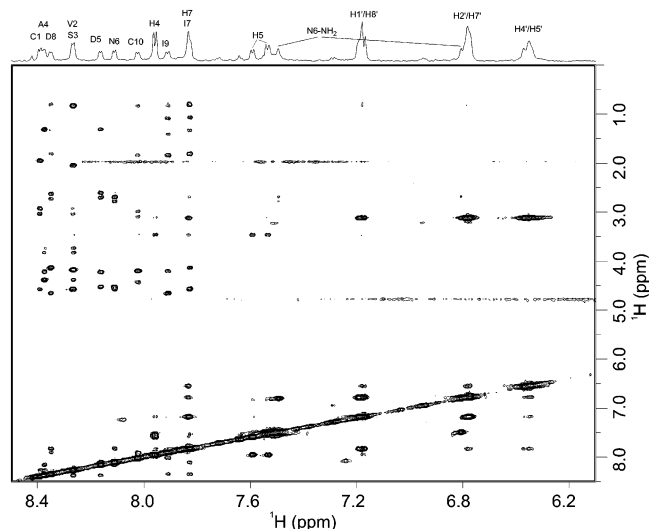


FIGURE 4: Downfield region of the 2-D NOESY spectrum (mixing time 800 ms) of pepF1-6R (50 μM) displaying the NOE connectivities involving rhodamine or polypeptide amide protons. Resonance assignments are indicated.

interactions between the rhodamines are observed. The complete NOESY spectrum, together with the 2-D TOCSY spectrum, revealed spin systems for the 10 amino acid residues. The assignments for these and the rhodamines are given in Table 1. Notably, chemical shift differences were either undetectable or very small for protons at the same positions on each rhodamine, suggesting that the two dye moieties on the labeled peptide were in similar environments. Several spectroscopic parameters indicate that the peptide does not adopt a single well-defined conformation; these were the limited chemical shift dispersion, absence of

Table 1: ^{1}H NMR Assignments for PepF1-6R and Rhodamine Signals

| residue | ^{1}H NMR Assignments | | | |
|---|---|---|---|---|
| | $H_N$ (ppm) | $H_\alpha$ (ppm) | $H_\beta$ (ppm) | other (ppm) |
| C1 | 8.39 | 4.57 | 3.05, 2.93 | |
| V2 | 8.26 | 4.19 | 2.06 | 0.84 |
| S3 | 8.26 | 4.38 | 3.83, 3.74 | |
| A4 | 8.37 | 4.22 | 1.32 | |
| D5 | 8.16 | 4.53 | 2.71, 2.62 | |
| N6 | 8.11 | 4.57 | 2.79, 2.69 | 6.80, 7.79 ($NH_2$) |
| I7 | 7.82 | 4.14 | 1.82 | 1.08, 0.81 |
| D8 | 8.35 | 4.66 | 2.74, 2.63 | |
| I9 | 7.91 | 4.20 | 1.85 | 1.09, 0.84, 0.80 |
| C10 | 8.02 | 4.44 | 3.11, 2.99 | |

| Rhodamine Signals | | | | | |
|---|---|---|---|---|---|
| proton(s) | chemical shift (ppm) | proton(s) | chemical shift (ppm) | proton(s) | chemical shift (ppm) |
| H-1′,8′ | 7.18[a] | H-4 | 7.96[a] | $H_N$[b] | 10.38, 10.43 |
| H-2′,7′ | 6.78[a] | H-5 | 7.53, 7.59 | $CH_2$[b] | 3.45, 3.46 |
| H-4′,5′ | 6.55[a] | H-7 | 7.82[a] | $CH_3$ | 3.06, 3.07 |

[a] NMR resonances for these proton sites in rhodamine moieties at each end of the decapeptide chain appeared at equivalent chemical shifts. [b] Linker.

Table 2: Proton−Proton Distances Derived from Cross-Peak Volumes Observed in 2-D NOESY Experiments

| proton A | proton B | NOE-derived distance (Å)[a] | distance in monomer structure (Å) | intermolecular distance in dimer model (Å) |
|---|---|---|---|---|
| H-4 | H-5 | | 2.5 | 15.3 |
| H-1′,8′ | H-2′,7′ | | 2.5 | 6.7 |
| H-1′,8′ | H-4′,5′ | 3.9 | 4.9 | 3.7 |
| H-2′,7′ | H-4′,5′ | 3.8 | 4.3 | 3.9 |
| H-1′,8′ | H-7 | 3.0 | 3.3 | 8.0 |
| H-2′,7′ | H-7 | 3.8[b] | 5.4 | 7.9 |
| H-4′,5′ | H-7 | 3.6 | 6.5 | 3.7 |

[a] These distances have an associated error of 0.3 Å, estimated from separate internal calibrations using the fixed distances between H-4 and H-5 and between the proton pairs H-1′(8′) and H-2′(7′), for a NOESY experiment recorded with a mixing time of 800 ms to provide acceptable cross-peak sensitivity. [b] The anomalously low NOE-derived distance between H-7 and H-2′(7′) is a consequence of a relayed effect via the short intramolecular distances between H-1′(8′) and H-2′(7′) and between H-7 and H-1′(8′), as confirmed by experiments at shorter mixing times (data not shown).

nonsequential NOE connectivities, and intermediate values (∼6 Hz) of the $H_N-H_\alpha$ scalar coupling constants (data not shown). NOE cross-peak volumes were used to derive approximate interproton distance restraints for the rhodamines, using a simple $r^{-6}$ relationship, and corrected for proton stoichiometry. Table 2 summarizes the interproton distances determined for the rhodamine component of pepF1-6R. These distances were used to model the structure of the rhodamine dimer, which is shown in Figure 5.

*Fluorescence Lifetimes*. Lifetime data were obtained on peptide samples before and after cleavage by Pronase. Peptide concentrations were ∼1 $\mu$M. Phase and modulation data are shown in Figure 6 for both pepF1-6R and pepF1-5R. Table 3 shows data from the nonlinear least-squares analysis based on discrete exponential decays. Before Pronase treatment, pepF1-6R and pepF1-5R each demonstrated a long lifetime component (2.44 ns for pepF1-5R and 2.50 ns for pepF1-6R) as well as short lifetime components (∼0.14 ns for pepF1-5R and ∼0.076 ns for pepF1-6R). In terms of the
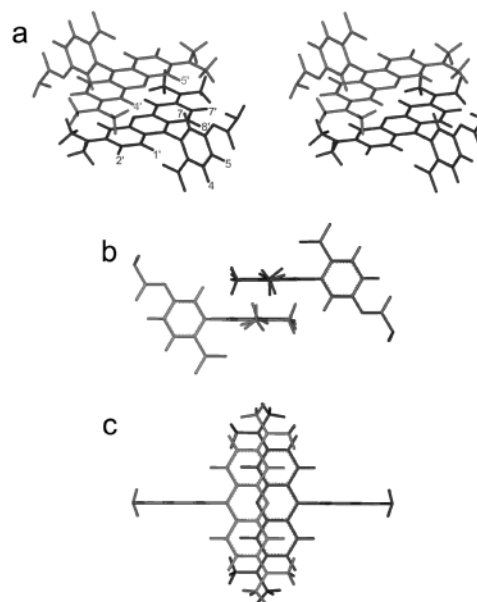


FIGURE 5: (a) Stereoview of the rhodamine dimer interface modeled on the basis of [1]H−[1]H distance restraints derived from NOE data. (b, c) Orthogonal views of the dimer interface illustrating the ring−ring separation and the extent of ring overlap.
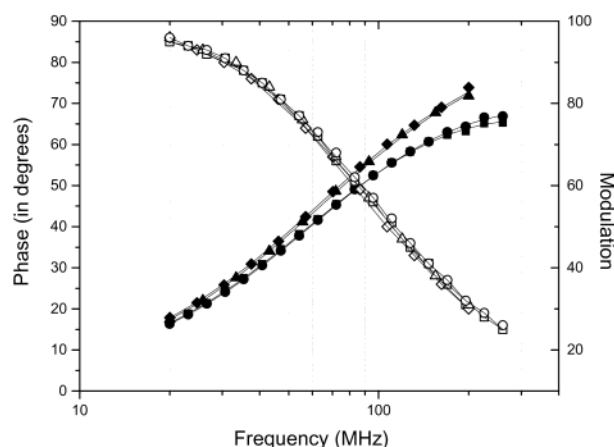


FIGURE 6: Typical phase (filled symbols) and modulation (open symbols) data for pepF1-5R before (circles) and after (triangles) Pronase treatment and for pepF1-6R before (squares) and after (diamonds) Pronase treatment.

Table 3: Fluorescence Lifetime Parameters of Intact and Cleaved Labeled Peptides[a]

| sample | $\tau_1$ (ns) | $f_1$ | $\alpha_1$ | $\tau_2$ (ns) | $f_2$ | $\alpha_2$ |
|---|---|---|---|---|---|---|
| pepF1-5R | 2.44 | 0.95 | 0.52 | 0.14 | 0.05 | 0.48 |
| pepF1-5R + Pronase | 2.43 | 1.00 | | | | |
| pepF1-6R | 2.50 | 0.95 | 0.37 | 0.076 | 0.05 | 0.63 |
| pepF1-6R + Pronase | 2.50 | 1.00 | | | | |

[a] Parameters $\tau_i$, $f_i$, and $\alpha_i$ denote the lifetime, fractional intensity, and relative molecular population of the *i*th species. In all cases, three data sets were taken, and the average values are given. Reduced $\chi^2$ values were between 0.3 and 1.5 and were calculated using nonlinear least-squares analysis assuming standard phase and modulation errors of 0.3° and 0.006, respectively, as previously described (*42*). In all cases the standard errors (67% confidence) were approximately ±0.02 ns for the lifetimes, ±0.01 for the fractional intensities, and ±0.06 for the preexponential ($\alpha$) terms.

fractional contribution to the total intensity (the *f* terms in Table 3), these short components accounted for only 5% of the emission in both cases. However, if one assumes that
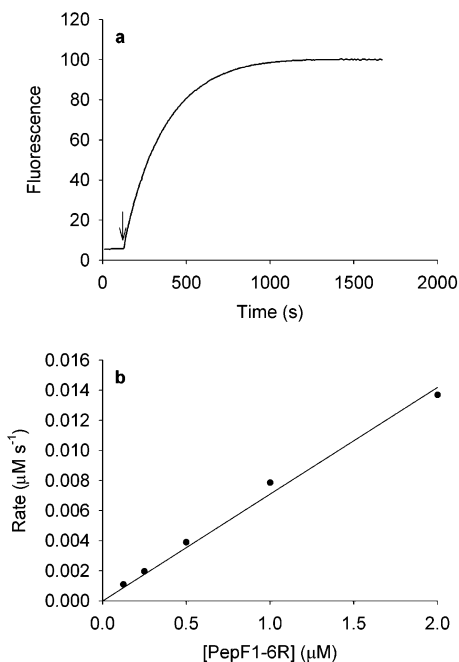
FIGURE 7: Hydrolysis of pepF1-6R by Pronase. (a) To a solution of 1.0 $\mu$M pepF1-6R in 0.35 mL of buffer at 20 °C was added 1.2 $\mu$g of Pronase in 1.4 $\mu$L of buffer. The point of Pronase addition is indicated with an arrow. Fluorescence emission was monitored with time. (b) Effect of concentration of pepF1-6R on its hydrolysis by Pronase. Initial rates from experiments as in (a) were calculated as described in Experimental Procedures and plotted against pepF1-6R concentration. The solid line is the best fit to a straight line.



FIGURE 8: Hydrolysis of pepF1-6R by PfSUB-1. (a) To a solution of 2.3 $\mu$M pepF1-6R in 80 $\mu$L at 37 °C was added 20 $\mu$L of ~0.7 $\mu$M PfSUB-1 (at ~200 s, denoted by an arrow). After sufficient data were collected to obtain the steady-state rate of hydrolysis (~900 s, denoted by an arrow), Pronase (1 $\mu$g in 5 $\mu$L) was added to cause complete hydrolysis. (b) Effect of concentration of pepF1-6R on its hydrolysis by PfSUB-1. Initial rates from experiments as in (a) were calculated as described in Experimental Procedures and plotted against pepF1-6R concentration. The solid line is the best fit to a straight line.

the quantum yields and lifetimes are proportional in these systems and also that excitation at 501 nm results in relative weights of dimer to monomer in proportion to their absorption spectra, then one can calculate preexponential factors ($\alpha$). These calculations indicate that the relative proportions of the molecular species associated with the short lifetime component (before Pronase treatment) were ~48% (pepF1-5R) and ~63% (pepF1-6R). Note that for the lifetime determinations, in contrast to the steady-state fluorescence measurements described above (Figure 3c,d), the background fluorescence from buffer containing NP-40 was less than 0.1% of the sample signal for either isomer, since excitation at 501 nm produced a significantly lower background than excitation at 550 nm. Approximately 1 h after Pronase treatment the lifetime measurements were repeated, and the 5- and 6-isomers exhibited single exponential decays of 2.43 and 2.50 ns, respectively.

*Kinetics.* Initial studies were made using the nonspecific cleavage of pepF1-6R by Pronase. Solutions (0.35 mL) of pepF1-6R ranging between 0.12 and 2.00 $\mu$M were incubated with Pronase (1.2 $\mu$g) at 20 °C, and the fluorescence intensity was recorded with time (Figure 7a). The initial rate of intensity increase was measured and converted to a rate of pepF1-6R cleavage based on knowledge of the total intensity change of the reaction and the initial concentration of pepF1-6R. The rate of cleavage of pepF1-6R was linearly dependent on [pepF1-6R] over the range measured (Figure 7b).

With the validity of this protease assay established with Pronase, similar kinetic measurements were made with PfSUB-1. In this case, pepF1-6R in digestion buffer (80 $\mu$L) was equilibrated at 37 °C, and recombinant PfSUB-1 (20 $\mu$L, containing 800 ng of purified protease) was added. A

slow linear increase in fluorescence intensity was observed (Figure 8a). After sufficient data to determine that the steady-state rate of intensity increase had accumulated, Pronase (1 $\mu$g) was added to enable a rapid determination of the end point of cleavage. The data were converted to a rate of pepF1-6R cleavage as described above. Again, there was a linear dependence of the rate of pepF1-6R cleavage on [pepF1-6R] over the measured concentration range (Figure 8b).

*Development of a Multiwell Assay.* As well as facilitating kinetic studies, the availability of a small synthetic fluorescent protease substrate allows the development of a simple assay capable of high-throughput screening for inhibitors of the protease. To explore the potential of pepF1-6R in such an assay, trial experiments were performed to optimize the conditions for a 96-well microtiter plate assay. Figure 9 shows the results of a typical assay in which PfSUB-1 at a series of concentrations was incubated for 18 h with a standard concentration (0.1 $\mu$M) of pepF1-6R in the microtiter format assay. At the highest concentration of protease used in this assay (0.1 $\mu$g mL$^{-1}$, approximately 2 nM protein; ref *3*), an 11.8-fold increase in fluorescence was obtained over the period of incubation. The fluorescence increase was approximately proportional to the concentration of protease used and was virtually completely ablated in the presence of the PfSUB-1 inhibitor pHMB.

## DISCUSSION

The initial motivation of our study was to develop a fluorogenic assay suitable for high-throughput screening of inhibitors of the protease PfSUB-1. However, the fluores-
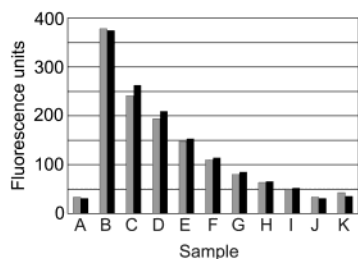
FIGURE 9: Multiwell assay of PfSUB-1 activity using pepF1-6R. Duplicate microtiter wells (each set of duplicates is shown as a pair of gray and black bars) containing a 0.2 $\mu$M solution of pepF1-6R were supplemented with an equal volume of buffer alone (A) or a solution of PfSUB-1 at a concentration of approximately 4 nM (B), 2 nM (C), 1 nM (D), 0.5 nM (E), 0.25 nM (F), 0.125 nM (G), 0.063 nM (H), 0.031 nM (I), or 0.015 nM (J) or 4 nM protease pretreated with 0.5 mM pHMB (K). Fluorescence values were measured after 18 h incubation at 37 °C.

cence enhancement we observed upon cleavage of our labeled substrate was up to twice as great as those found in related studies, where maximum enhancements of 15-fold have been reported (*4, 5*). The favorable signal amplitude of the present system prompted us to undertake more detailed characterization of the fluorogenic substrate. A particular point of interest in the present system is the geometry of the rhodamine−rhodamine interaction that underlies the fluorescence quenching.

Spectral shifts due to dye aggregation have been known and studied for almost a century (*18*). Specific studies on rhodamines were first carried out by Förster (*6*), and these and other data were eventually interpreted in terms of exciton models (see, for example, refs *19−21*). More recently, ground-state xanthene dimer formation has been used to study protein−protein interactions (*22−24*) and hairpin interactions in oligonucleotides (*25*), as well as being applied in protease assays (*4, 5*). Packard et al. proposed, for their particular doubly rhodamine-labeled peptide, an essentially planar, edge-to-edge association of the xanthene rings (*4*), and they have described several further studies predicated on this geometry (*26−29*). The rationalization for the edge-to-edge model was based on optical spectroscopy. The authors proposed that an observed red shift of the 353 nm peak, upon dimer formation, considered together with the blue shift of the 552 nm band, could best be explained by exciton theory if the dimer formed in an edge-to-edge manner. Their paper did not specify the magnitude of the red shift in the 353 nm region, so direct comparisons with our spectra are not possible. As mentioned earlier, the spectral shifts in the 353 nm region upon dimer formation in our systems depended upon the isomer utilized. We also note the study by Gakamsky et al. (*24*) using the similar rhodamine Texas Red, where changes in the visible absorption bands were completely analogous to those observed in our work but no shifts were evident in their published data for the mid-UV absorption band.

While it is possible that the particular peptide length and sequence used in the study by Packard et al. (*4*) may impose specific constraints, the edge-to-edge association has not been previously reported for rhodamines. X-ray crystal structures of rhodamines show face-to-face packing in the unit cell although these could be influenced by crystal lattice forces (*30, 31*). More relevant examples are a crystal structure of rhodamine dimers in the binding site of a Bence−Jones

protein, where the dye is in a protein environment and in the presence of lattice water (*32*), and an NMR study of rhodamine dimers in aqueous solution (*33*). Both studies show a stacked arrangement of the xanthene rings with the carboxy groups on the pendant phenyl rings projecting outward from the dimer core. The stacked geometry places particular protons of one rhodamine in proximity with nonisochronous protons on the partner rhodamine in the dimer, allowing determination of NOE effects and thus of distance constraints.

The interproton distances derived for pepF1-6R from NMR measurements shown in Table 2 are compared with the same interproton distances in a monomer. Table 2 also lists the relevant interproton distances for the optimized dimer model. Examination of a series of NOESY spectra recorded with different mixing times served to distinguish between direct and relayed NOE effects. Relayed effects, especially between ortho-related protons in aromatic rings, become significant at extended mixing times and explain the anomalous cross-peak seen in Figure 4 for an apparent NOE between H-7 and H-2′,7′ of the paired rhodamines (see footnotes to Table 2). The differences between the NOE and monomer-derived distances can be reconciled by invoking a mode of intramolecular dimerization that has a typical stacked relationship of the xanthene rings, with a ring−ring separation of ∼3.5 Å, similar to that described for aqueous solutions of rhodamine homo- and heterodimers (*33*), and a horizontal offset of the xanthene ring centroids by ∼2.1 Å (Figure 5). Our data are incompatible with a model involving coplanar arrangement of the xanthene groups, with dimerization via an edge-to-edge interaction. In particular, observation of a significant NOE between H-4′(5′) and H-7 dictates a stacked arrangement, as the minimum H-4′(5′) to H-7 separation in an edge-on dimer would be 6.5 Å, i.e., the distance in the isolated monomer as a lower limit. The absence of any observable NOE between H-4′(5′) and H-7 in such circumstances was confirmed using 1-D steady-state NOE experiments on 6-CATR in CDCl$_3$−MeOH-$d_4$, under which conditions the dye is entirely monomeric (data not shown). Thus, at least in the present 6-labeled substrate, the rhodamine dimer geometry experimentally determined is best fit by a stacked model as opposed to an edge-to-edge one.

The fluorescence lifetime data indicate that in the uncleaved peptides a significant portion (∼52% in pepF1-5R and ∼37% in pepF1-6R) of the rhodamine moieties may remain in the unquenched (monomeric) conformation. This estimation is prone to error since (a) it is based on the assumption that the quantum yield and lifetime are proportional, which may not be the case given the large change in the absorption spectrum, (b) small errors in the lifetime of the quenched component will significantly impact on the calculation of the preexponential term, and (c) the excitation spectra of the monomeric and dimeric rhodamines likely have different maxima (*24*) so the fluorescence intensities based on single-wavelength excitation measurements may not accurately reflect the relative proportions of species present. Nevertheless, the data strongly suggest the presence of an equilibrium between dimer and monomer rhodamine states for both peptides. This equilibrium must be rapid on the NMR time scale since only a single set of resonances was observable for pepF1-6R. The fluorescence results further suggest that the combination of peptide flexibility and

intrinsic free energy of the rhodamine interaction was such that the dimer formation is more favored for the 6-isomer than for the 5-isomer. However, precise determination of the equilibrium constants for these systems is hampered because of uncertainties in the proportions of the two forms, as outlined above. Differences between the molecular arrangement within the rhodamine dimers were also evident from the fact that the resolved lifetime of the short component was lower in the case of pepF1-6R (0.076 ns) compared to pepF1-5R (0.14 ns). It is difficult to compare our lifetime results with those of Kemnitz and Yoshihara (8), who studied a series of rhodamine compounds in nonaqueous solvents. However, they did attribute a subnanosecond component to fluorescence of the dimer. The lifetime differences between pepF1-5R and -6R are paralleled by differences in the respective absorption spectra, specifically the differences in the mid-UV absorption and the different intensity ratios for the two visible peaks (518 and 549 nm) for pepF1-5R and -6R described above. The latter also suggest that the 6-isomer favors dimer formation. However, a complementary structural determination for pepF1-5R was beyond the scope of the present study.

The study by Packard et al. (4) proposed that it was desirable to incorporate "conformation-determining" regions into the peptide sequence in order to promote efficient interaction of the rhodamine monomers. However, a later study by the same group showed that incorporation of flexible linker arms generally promoted dimerization, leading to better fluorescence quenching (28). The related study by Geoghegan et al. (5) also suggested that conformation-determining regions in the peptide are not required, and our work agrees with that conclusion. Indeed, our NMR data indicate that the peptide sequence in pepF1-6R is unstructured, as would generally be expected for a small peptide. This is important, since it suggests that there is little restriction on the peptide sequence that may be used in such substrates, in turn indicating that the approach has wide application for design of fluorogenic protease substrates.

Most existing fluorogenic peptide substrates for proteases incorporate a C-terminal fluorescent group (most commonly a 7-aminocoumarin) linked in an amide bond, cleavage of which generates the fluorescence increase as the free fluorophore is released (e.g., ref 34). The utility of this class of substrates can be limited, since the presence of a bulky fluorophore directly adjacent to the scissile bond can often interfere with substrate recognition. In addition, for efficient substrate recognition, many proteases require interaction with residues on both the P and P′ sides of the scissile bond, as in their physiological protein substrate(s). The inclusion of a sequence which can interact with both the S and S′ subsites of the protease often enhances the selectivity (reflected by the $k_{cat}/K_M$ ratio) of a protease substrate. To accommodate this, a second class of fluorescent substrates is available, which use FRET to quench the fluorescence of a terminal group in the intact peptide. The general structures of the two most commonly used of these are DABCYL-(Xaa)$_n$-EDANS and Abz-(Xaa)$_n$-3-nitrotyrosine, where (Xaa)$_n$ is any amino acid sequence, and numerous other donor/acceptor pairs have also been explored (e.g., refs 35−39). In all cases the efficiency of intramolecular quenching is critically dependent on the distance between the donor and acceptor moieties. For efficient quenching in the EDANS/DABCYL system,

for example, $n$ should not exceed 11 or 12; quenching efficiency at this distance is only about 10-fold (39). Our data and those of Geoghegan et al. (5) suggest that substrates based on the approach reported here are not subject to such restrictions in the length of the linking peptide; indeed, the latter authors demonstrated that an intervening sequence of up to 18 residues in length did not prevent efficient dimerization of terminal tetramethylrhodamine moieties (5). This is an important consideration when the precise S and S′ subsite requirements of a protease are unknown. Furthermore, and perhaps more important, synthesis of the doubly labeled peptide is relatively simple, due to the requirement only to incorporate an identical group at each of the two available reactive cysteine side chains; synthesis of FRET-based substrates is significantly more complex, usually requiring incorporation of the donor and acceptor groups during solid-phase synthesis (e.g., ref 36).

Synthesis of the fluorogenic peptide by labeling cysteine residues rather than N-terminal amines and/or $\epsilon$-amino groups on lysine allows for the presence of lysines within the target sequence of other potential fluorogenic peptides of this general type without a need for more complex chemical strategies. The use of iodoacetamidorhodamines rather than maleimidorhodamines (5) for labeling may also be beneficial, since it does not create new stereo centers. In principle, dual labeling by a maleimide reagent of a peptide that contains two cysteines will result in four diastereoisomeric species, each of which could have different properties. At least one well-characterized example of diastereoisomers being formed upon labeling a cysteine residue with a maleimide reagent has been described (40).

Alternative approaches based on a similar principle may be taken. For example, Wei et al. used a fluorescein−rhodamine heterolabeled 13-mer peptide to study antibody binding. Fluorescence quenching in this case was mediated by a combination of ground-state and excited-state effects. Binding of the labeled peptide to a specific antibody resulted in an ∼8-fold increased rhodamine fluorescence that was attributed to dissociation of intramolecular dimers (41). With a suitable bridging peptide sequence, such peptides could also be used as fluorogenic protease substrates.

At concentrations up to 5 $\mu$M there was a linear relationship between the concentration of pepF1-6R and the initial rate of its cleavage by recombinant PfSUB-1, indicating that the $K_M$ for this substrate is substantially higher than 5 $\mu$M. This is consistent with previous studies of cleavage by recombinant PfSUB-1 of an unlabeled peptide substrate, Ac-LVSADNIDIS-OH, where the experimentally determined $K_M$ value was ∼770 $\mu$M (3). If of a similar order of magnitude, experimental determination of the $K_M$ for pepF1-6R would be very difficult, since at such concentrations quenching effects due to intermolecular dimerization might become significant and inner filter effects would come into play. Such problems are also a feature of FRET-based systems (e.g., refs 36, 38, and 39).

We have shown that pepF1-6R can be used in a microtiter plate assay suitable for scale-up to high-throughput format, thus facilitating screens of large libraries of potential inhibitors, and this has been successfully implemented (K. Ansell, B. Saxty, C. Kettleborough, and M. J. Blackman, unpublished). The results also show that interaction of the tetramethylrhodamine dye monomers in pepF1-6R is unaf-

fected between pH 5 and pH 10, allowing the substrate to be used for analyzing the pH dependence of PfSUB-1 activity over at least this range. Both pepF1-6R and pepF1-5R may also have applications for exploring the activity of PfSUB-1 in situ in the malaria merozoite, where the enzyme accumulates in secretory granules; preliminary experiments suggest that the substrates are readily membrane permeable, and cleavage of the intracellular compound may allow visualization of these organelles by fluorescence microscopy.

## REFERENCES

1. Blackman, M. J. (2000) *Curr. Drug Targets 1*, 59−83.
2. Sajid, M., Withers-Martinez, C., and Blackman, M. J. (2000) *J. Biol. Chem. 275*, 631−641.
3. Withers-Martinez, C., Saldanha, J. W., Ely, B., Hackett, F., O'Connor, T., and Blackman, M. J. (2002) *J. Biol. Chem. 277*, 29698−29709.
4. Packard B. Z., Toptygin, D. D., Komoriya, A., and Brand, L. (1996) *Proc. Natl. Acad. Sci. U.S.A. 93*, 11640−11645.
5. Geoghegan, K. F., Rosner, P. J., and Hoth, L. R. (2000) *Bioconjugate Chem. 11*, 71−77.
6. Förster, T., and König, E. (1957) *Z. Elektrochem. 61*, 344−348.
7. Arbeloa, I. L., and Ojeda, P. R. (1982) *Chem. Phys. Lett. 87*, 556−560.
8. Kemnitz, K., and Yoshihara, K. (1991) *J. Phys. Chem. 95*, 6095−6104.
9. Corrie, J. E. T., and Craik, J. S. (1994) *J. Chem. Soc., Perkin Trans. 1*, 2967−2973.
10. Braunschweiler, L., and Ernst, R. R. (1983) *J. Magn. Reson. 53*, 521−528.
11. Jeener, J., Meier, B. H., Bachmann, P., and Ernst, R. R. (1979) *J. Chem. Phys. 71*, 4546−4553.
12. Piotto, M., Saudek, V., and Sklenar, V. (1992) *J. Biomol. NMR 2*, 661−665.
13. States, D. J., Haberkorn, R. A., and Ruben, D. J. (1982) *J. Magn. Reson. 48*, 286−292.
14. Delaglio, F., Grzesiek, S., Vuister, G. W., Zhu, G., Pfeifer, J., and Bax, A. (1995) *J. Biomol. NMR 6*, 277−293.
15. Spencer, R. D., and Weber, G. (1969) *Ann. N.Y. Acad. Sci. 158*, 361−376.
16. Spencer, R. D., and Weber, G. (1970) *J. Chem. Phys. 52*, 1654−1663.
17. Jameson, D. M., and Hazlett, T. L. (1991) in *Biophysical and Biochemical Aspects of Fluorescence Spectroscopy* (Dewey, G., Ed.) pp 105−133, Plenum Press, New York.
18. Sheppard, S. E. (1909) *Proc. R. Soc. London, Ser. A 82*, 256−270.
19. Kasha, M. (1963) *Radiat. Res. 20*, 55−71.
20. Hochstrasser, R. M., and Kasha, M. (1964) *Photochem. Photobiol. 3*, 317−331.
21. Kasha, M., Rawls, H. R., and El-Bayoumi, M. A. (1965) *Pure Appl. Chem. 11*, 371−392.
22. Hamman, B. D., Oleinikov, A. V., Jokhadze, G. G., Bochkariov, D. E., Traut, R. R., and Jameson, D. M. (1996) *J. Biol. Chem. 271*, 7568−7573.
23. Traut, R. R., Debendranath, D., Bochkariov, D., Oleinikov, A. V., Jokhadze, G. Hamman, B. D., and Jameson, D. M., (1995) *Biochem. Cell Biol. 73*, 949−958.
24. Gakamsky, D. M., Davis, D. M., Haas, E., Strominger, J. L., and Pecht, I. (1999) *Biophys. J. 76*, 1552−1560.
25. Bernacchi, S., and Mély, Y. (2001) *Nucleic Acids Res. 29*, e62.
26. Packard, B. Z., Komoriya, A., Toptygin, D. D., and Brand, L. (1997) *J. Phys. Chem. B 101*, 5070−5074.
27. Packard, B. Z., Toptygin, D. D., Komoriya, A., and Brand, L. (1997) *Biophys. Chem. 67*, 167−176.
28. Packard, B. Z., Toptygin, D. D., Komoriya, A., and Brand, L. (1997) *J. Phys. Chem. B 102*, 752−758.
29. Packard, B. Z., Komoriya, A., Nanda, V., and Brand, L. (1997) *J. Phys. Chem. B 102*, 1820−1827.
30. Abrams, M. J., Picker, D. H., Fackler, P. H., Lock, C. J. L., Howard-Lock, H. E., Faggiani, R., Teicher, B. A., and Richmond, R. C. (1986) *Inorg. Chem. 25*, 3980−3983.
31. Corrie, J. E. T., Moore, M. H., and Turkenburg, J. P. (2002) unpublished data.
32. Edmundson, A. B., Ely, K. R., and Herron, J. N. (1984) *Mol. Immunol. 21*, 561−576.
33. Ilich, P., Mishra, P. K., Macura, S., and Burghardt, T. P. (1996) *Spectrochim. Acta A 52*, 1323−1330.
34. Backes, B. J., Harris, J. L., Leonetti, F., Craik, C. S., and Ellman, J. A. (2000) *Nat. Biotechnol. 18*, 187−193.
35. Yaron, A., Carmel, A., and Katchalski-Katzier, E. (1979) *Anal. Biochem. 95*, 228−235.
36. Grahn, S., Ullmann, D., and Jakubke, H. (1998) *Anal. Biochem. 265*, 225−231.
37. Meldal, M., and Breddam, K. (1991) *Anal. Biochem. 195*, 141−147.
38. Jean, F., Basak, A., DiMaio, J., Seidah, N. G., and Lazure, C. (1995) *Biochem. J. 307*, 689−695.
39. Holskin, B. P., Bukhtiyarova, M., Dunn, B. M., Baur, P., de Chastonay, J., and Pennington, M. W. (1995) *Anal. Biochem. 227*, 148−155.
40. Hirshberg, M., Henrick, K., Haire, L. L., Vasisht, N., Brune, M., Corrie, J. E. T., and Webb, M. R. (1998) *Biochemistry 37*, 10381−10385.
41. Wei, A. P., Blumenthal, D. K., and Herron, J. N. (1994) *Anal. Chem. 66*, 1500−1506.
42. Jameson, D. M., Gratton, E., and Hall, R. D. (1984) *Appl. Spectrosc. Rev. 20*, 55−106.

BI0263661